Geologica Acta, Vol.16, Nº 4, December 2018, 375-390
DOI: 10.1344/GeologicaActa2018.16.4.3

geologica acta

The extent of penetrative Pyrenean deformation in the Ebro foreland Basin: Magnetic fabric data from the eastern sector

J.M. PARÉS[1] and D. ANASTASIO[2]

[1]**Geochronology & Geology Program, CENIEH**
Paseo Sierra de Atapuerca 3, 09002 Burgos, Spain

[2]**Earth and Environmental Sciences Department, Lehigh University**
1 West Packer Ave, Bethlehem, PA, 18015, USA

ABSTRACT

We studied Cenozoic sedimentary rocks in the NE Ebro foreland Basin using the Anisotropy of Magnetic Susceptibility (AMS) as a proxy for grain preferred orientation. Our new data, in combination with existing results, reveal that penetrative strain by layer-parallel shortening extends well beyond the Pyrenean thrust-wedge front into the Ebro foreland Basin, challenging the concept of the location of "deformation front" in the Southern Pyrenees. Penetrative strain, as revealed by the magnetic fabrics, seems to reach larger distances into the Ebro foreland Basin where stiffer layers constitute the main detachment level, whereas to the East strain dissipates closer to the deformation front when the detachment is mostly due to salt deposits.

KEYWORDS **South-Pyrenean frontal thrust. Anisotropy of Magnetic Susceptibility. Cenozoic. Layer parallel shortening.**

INTRODUCTION

Deformation is critical to understanding the dynamic Earth and mountain building. Convergence at plate boundaries is responsible for the growth of most mountain ranges on Earth, where contractional strains deform the crust producing folds and faults that shorten and thicken the lithosphere. Rock deformation in such convergent zones decays away from the topographic mountain front to where no contractional structures are observed in the foreland (*e.g.* Lacombe and Mouthereau, 1999). However, when appropriate proxies for penetrative deformation are used, it becomes apparent that horizontal shortening extends well beyond the thrust front in most forelands, leading us to re-consider the concept of the location of the "deformation front" in orogens. For example, the concept of "tectonite front" was born to refer to the onset of a preferred crystallographic orientation (Fourmarier, 1923; Fellows, 1943), although the challenge in determining crystallographic fabrics has prevented the broad usage of such concept. Instead, the notion of "cleavage front", observable at mesoscopic scale has been more widely used as far as establishing the deformation front in orogens (*e.g.* Holl and Anastasio, 1995). The Anisotropy of Magnetic Susceptibility (AMS) is possibly the most sensitive proxy for penetrative rock deformation at the microscale, as it is able to sense feeble grain preferred orientation in rocks where no deformation appears at the mesoscopic scale (*e.g.* Kissel *et al.*, 1986; Aubourg *et al.*, 1991; Tarling and Hrouda, 1993 and references therein). AMS has evidenced that Layer Parallel Shortening (LPS) extends well beyond the observed deformation front in foreland basins (*e.g.* Parés *et al.*, 1999). In this study we report and discuss new and existing AMS results from different locations in the Ebro foreland Basin that help us understanding the development of penetrative deformation in Cenozoic sedimentary rocks in the Southern Pyrenean foreland Basin.

METHODS

Anisotropy of Magnetic Susceptibility (AMS): Principles

Rock-forming minerals are magnetically anisotropic in that the magnetic susceptibility (or K=M/H, M: ratio of magnetization to the applied field H) is directionally dependent. The so-called AMS defines a symmetric, second-rank tensor that has six independent matrix elements. When the coordinate system is referred to the eigenvectors, these trace an ellipsoid that is known as the magnitude ellipsoid (Nye, 1957) whose semi-axes are the three principal susceptibilities ($K_{max} \geq K_{int} \geq K_{min}$). An intrinsic property of most of rock-forming minerals is that their magnetic susceptibility is anisotropic (Nye, 1957) and thus $K_{ij}=M_i/H_j$. For example, it has been demonstrated that magnetic axes in biotite crystals conform to the density distributions of mineral lattice planes obtained by x-ray goniometry (Richter *et al*., 1993, Schmidt *et al*., 2009). These results reveal that densities from x-ray for chlorite and mica are perfectly reflected by the distribution of the minimum susceptibility axes. The study by Richter *et al*. (1993) was possibly the first demonstration that the normalized magnetic parameters ($M_i=\ln(K_i/[K_{max}*K_{int}*K_{min}]^{1/3})$) correlate directly with March strains as obtained from x-ray texture goniometry. The study was an important step forward showing the AMS as a sensitive and rapid gauge for bulk crystallographic preferred orientation in rocks, with the advantage of using large sample volumes (typically about $1lcm^3$), as opposed to the essentially two-dimensional slice used in optical and x-ray methods.

As far as the source of magnetic susceptibility, whereas ferromagnetic, moderate to high susceptibility minerals (*e.g*. magnetite, hematite) are minor components in most pelitic rocks, the dominant mineralogy corresponds to paramagnetic, lower magnetic susceptibility phases. Indeed, the average value of bulk magnetic susceptibility of mudrocks (10^{-4}–10^{-5}SI) suggests that the concentration of iron oxides such as magnetite is typically less than 0.01wt.% (*e.g*. Parés, 2015) which is consistent with the dominance of paramagnetic susceptibility in mudrocks. Numerous rock-magnetic studies where paramagnetic and ferromagnetic susceptibilities have been quantified revealed that typically the former dominates in mudstones (*e.g*. Martín-Hernández and Hirt, 2001 and references therein), therefore the AMS is dominated by the paramagnetic component, and most specifically by the shape anisotropy of clay minerals although very fine magnetic particles attached to the clay fabric might also contribute (Kodama and Sun, 1992).

AMS has been shown to have great potential in tracking early deformation stages in anchimetamorphic grade rocks (Robion *et al*., 1995, 1997, 1999; Lüneburg *et al*., 1999; Gil-Imaz *et al*., 2000; Parés and van der Pluijm, 2003; Debacker *et al*., 2004; Hirt *et al*., 2004). Although Borradaile and Tarling (1981) reported results from "weakly deformed slates", the study by Kissel *et al*. (1986) is possibly the first to demonstrate the great potential of AMS in weakly deformed rocks, as these authors showed that by using this technique it is possible to detect very subtle deformation in mudstones otherwise seemingly undeformed. Further contributions by Aubourg *et al*. (1991); Averbuch *et al*. (1992); Owens (1993); Parés and Dinarès-Turell (1993); Sagnotti and Speranza (1993); Collombat *et al*. (1995); Parés *et al*. (1999); Sagnotti *et al*. (1999); Anastasio *et al*. (2015) (also see Borradaile and Jackson, 2004 for a review) take advantage of the sensitivity of AMS to identify and define the orientation of weak tectonic magnetic fabrics. In most of these examples, the studied mudrocks are uncleaved, typically flat-lying, and macroscopically undeformed. Despite the field appearance of these mudrocks, a subtle, weak tectonic fabric is observed when using magnetic anisotropy methods. In an effort to merge all these models for fabric development arising from tectonic deformation with magnetic fabrics, Parés *et al*. (1999) proposed a pattern for progressive stages in AMS evolution in strained mudrocks, complementing the previous models envisioned by Averbuch *et al*. (1992) and Bakhtari *et al*. (1998). The model includes four type of magnetic fabrics that develop in weakly deformed mudrocks undergoing progressive deformation and has subsequently been observed and adopted in later studies of similar rock types (Frizon de Lamotte *et al*., 2002; Souqué *et al*., 2002; Saint-Bezar *et al*., 2002; Sans *et al*., 2003; Aubourg *et al*., 2004; Larrasoaña *et al*., 2004; Robion *et al*., 2007; Oliva-Urcia *et al*., 2009; Soto *et al*., 2009; Weil and Yonkee, 2009; Mochales *et al*., 2010; Pueyo-Anchuela *et al*., 2010; Kanamatsu *et al*., 2012). All these studies highlight that AMS is a proxy for fabric and strain in that it records preferred grain orientation in sedimentary rocks even before the appearance of weakly penetrative cleavage. The deformation pathway represented in Figure 1 summarizes the magnetic fabric path of siliciclastic rocks under progressive deformation (layer parallel shortening).

A summary of the AMS studies in deformed mudrocks where paramagnetic phyllosilicates control the fabric is as follows (Parés, 2015):

i) Principal axes of maximum susceptibility (K_{max}) are particularly sensitive to tectonic shortening, as they develop a magnetic lineation that mimics the intersection of bedding and tectonic flattening plane (the strain XY plane).

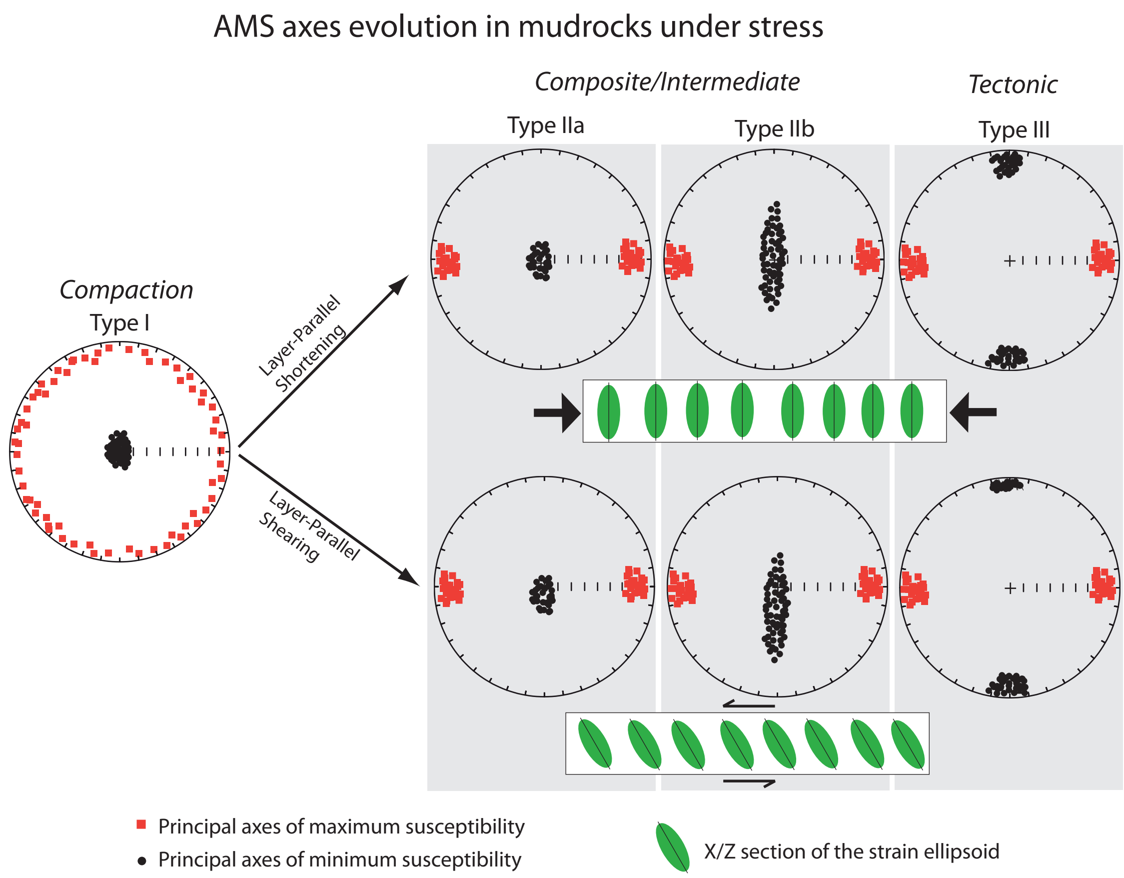

FIGURE 1. Conceptual model of Anisotropy of Magnetic Susceptibility (AMS) development in mudrocks undergoing progressive deformation (modified from Parés, 2015) (squares: principal maximum susceptibility axes (K_{max}); dots: principal minimum susceptibility axes (K_{min}); Green ellipse: strain ellipse). Type I fabric is essentially a compaction, sedimentary fabric with K_{min} axes normal to the deposition plane and K_{max} axes scatter along it. Type II (a and b) fabric reveals the imprint of the first lateral shortening on the initial sedimentary fabric where both the Layer Parallel Shortening (LPS) or flattening plane and depositional plane compete to define the total magnetic fabric. K_{max} axes parallel the intersection direction between these two planes. K_{min} axes eventually show a girdle that is parallel to the maximum shortening direction. Ultimately K_{min} axes become parallel to the shortening direction and K_{max} axes remain parallel to the intersection direction and not necessarily to the maximum extension direction (Type III). Rocks deformed by layer-parallel shearing, Types IIa and IIb ellipsoids show a girdle of K_{min} axes that are plunging away from the tectonic extension direction.

ii) Layer parallel shortening extends well beyond the “deformation front” in orogenic settings.

iii) An intermediate fabric (Type IIa and IIb) is very common where bedding and flattening planes compete to define the finite magnetic anisotropy ellipsoid.

A corollary of all these existing results is that because AMS in weakly deformed rocks senses preferred grain orientation (mostly from phyllosilicate grains), grain slippage and rotation must have occurred to develop such tectonic fabric. Early studies have already experimentally documented that strain causes parallel orientation of platy minerals perpendicular to the direction of shortening (*e.g.* Sorby, 1908; Clark, 1970; Fernández, 1987). Still, what requires further research are the implications of such grain sliding and rotation, as they require a reduction in shear strength in order to facilitate the grains to slide past each other. These aspects need still to be further investigated.

Data acquisition

AMS was measured on a 1-FA Kappabridge (AGICO Instruments), a fully automated inductive bridge, at a frequency of 976Hz and a field of 200A/m, at the Geochronology Laboratory of the CENIEH (Burgos, Spain). The instrument measures the susceptibility of a slowly spinning specimen. The operator has to adjust the specimen only in three perpendicular positions. The measurement takes about 2 minutes per specimen and is very precise, due to many susceptibility determinations in each plane perpendicular to the axis of specimen rotation. Special software combines the measurements in three perpendicular planes plus one bulk value to create a complete susceptibility tensor. The errors in determination of this tensor are estimated using a method based on multivariate statistics principles Jelinek (1978). There is a plethora of parameters to describe the axial magnitude relationships of the susceptibility ellipsoid (see also Tarling and Hrouda, 1993; Tauxe, 1998). The simplest expressions are the axial ratios L (K_{max}/K_{int}) (Balsley and Buddington, 1960), F (K_{int}/K_{min}) (Stacey *et al.*, 1960) and P (K_{max}/K_{min}) (Nagata, 1961). Alternatively, other authors use the parameters P' ($P'=\exp 2(a_1^2+a_2^2+a_3^2)]^{1/2}$ (Jelinek, 1981) where $a_1=\ln(K_{max}/K_b)$, etc. and $K_b=(K_{max}+K_{int}+K_{min})/3$ (Nagata, 1961) to express the fabric intensity as a measure of eccentricity and T ($T=2(\ln K_{int}-\ln K_{min})/[\ln K_{max}-\ln K_{min}]-1$) (Jelinek, 1981) to define the degree to which the ellipsoid is oblate or prolate, both adopted in this study.

Layer-Parallel-shortening and Penetrative Strain

Layer-Parallel Shortening (LPS) in fold-and-thrust belts can be regarded as the mechanism by which the layers above a décollement accommodate the decreasing displacement forelandward away from the mountain front (Engelder and Engelder, 1977; Cooper *et al.*, 1983; Williams and Chapman, 1983; Geiser, 1988; Evans and Dunne, 1991; Lacombe and Mouthereau, 1999; Koyi *et al.*, 2004; Tavani *et al.*, 2015). Nickelsen (1983) noticed LPS in the Appalachians thanks to deformed fossils, and he referred as to "lateral compaction". Penetrative Strain (PES) includes microscale LPS mechanisms, and its distribution during a deformation sequence is not yet well understood (*e.g.* Burberry, 2015). Also, the extent to which penetrative strain and hence LPS depend on the décollement tip still remains an open question. The importance of including the penetrative strain in, for example, balanced cross-sections has become apparent (Hossack, 1978; Woodward *et al.*, 1986; Mitra, 1990; Homza and Wallace, 1997). A number of studies indicate that balanced cross-sections that consider macroscopic structures alone can underestimate cumulative shortening (*e.g.* Mitra, 1994; McNaught and Mitra, 1996; Yonkee and Weil, 2009). Layer-parallel shortening magnitudes vary significantly, typically between *ca.* 5 and 30%, so LPS encompasses a high percentage of the total deformation in some cases, and depends strongly on the mechanical strength of the strata being deformed (Crosby, 1969; Engelder, 1979; Nickelsen, 1983; Craddock, 1992; Mitra, 1994; McNaught and Mitra, 1996; Mukul and Mitra, 1998; Faill and Nickelsen, 1999; Yonkee and Weil, 2009). Tavani *et al.* (2006; 2008; 2011) reported pressure solution cleavage that accounts for 80% of the total shortening. It follows that the development and distribution of PES is of importance to balance cross-sections, for total shortening estimates, and in addition it has implications on the porosity and permeability of reservoirs. AMS can reveal penetrative strain at the scale of 10cc or even less, and therefore is an unprecedented proxy for establishing and potentially quantifying PES in sedimentary rocks (see review in Parés, 2015).

GEOLOGICAL SETTING

In the Eastern Pyrenees along the footwall of the Vallfogona Thrust, continental sediments of the Ebro foreland Basin include the Berga Formation (Fm.) conglomerates (Riba, 1973; Puigdefàbregas *et al.*, 1986, 1992) (Fig. 2). To the South, the Berga conglomerates become progressively finer grained and thinner bedded and grade into the fluvial conglomerates, sandstones, and claystones of the Solsona Fm. (Saez, 1987; Saez *et al.*, 2007; Barrier *et al.*, 2010). The footwall of the Vallfogona thrust exposes a spectacular, regional-scale, growth fault-propagation fold in the syntectonic Berga conglomerates. At a regional scale, unconformity geometries vary from angular to the West at Serres de Lord to progressive East of Serres de Busa. Across the structure, bedding dips change from 70° overturned to upright and horizontal over a few kilometers of section (Fig. 3). In a classic study, Riba (1976) defined "progressive unconformities" or cumulative wedge systems at this location and showed that they developed on a tilting depositional surface when the sediment accumulation rate is higher than uplift. Williams *et al.* (1998) have thoroughly studied the depositional genesis of the Berga Fm. growth section and showed that the growth of the Puig-reig anticline and Busa syncline was unsteady based on relative dating. Balanced and restored cross sections and forward geometric modeling by Ford *et al.* (1997), Suppe *et al.* (1997) and later Alonso *et al.* (2011) agree on the geometry of the fault propagation fold pair but not on all the kinematic details. Kinematic uncertainty remains as to whether limb rotation or limb lengthening produced the fold amplification during fault slip, although Carrigan *et al.* (2016) argue for a fixed limb length.

Just North of the town of Sant Llorenç de Morunys (Fig. 4), the Berga Conglomerates lie conformably on the marine marls and marly limestones assigned to the Bartonian-Lower Priabonian (Solé-Sugrañes and Mascareñas, 1970). Magnetostratigraphic results (Carrigan *et al.*, 2016; Parés *et al.*, 2016) reveal that the Berga Conglomerates have an age of Eocene-Oligocene and that the onset of deformation of the growth strata occurred at 33.85Ma.

Further South of Busa syncline there is a set of long-wavelength anticlines and associated synclines, with an oblique trend to the Pyrenean direction, mostly formed as ramp anticlines (Fig. 2). In the southern area, a thrust wedge related to salt tectonics or triangle zone is defined by folds and faults striking NW-SE (*e.g.* Puig-reig anticline, Solsona), and SW-NW to WSW-ENE (Cardona Salt unit, El Guix anticlines) (Figs. 2; 4). The Southern Pyrenean Triangle Zone (Sans *et al.*, 1996) dies out to the E and to the W where the thrust front emerges. The tip line of the thrust front is considered to be located 40km South of the South Pyrenean Main Thrust (Vergés *et al.*, 1992). The orientation of the frontal thrust wedge is controlled by the southern pinch-outs

Geologica Acta, 16(4), 375-390 (2018)
DOI: 10.1344/GeologicaActa2018.16.4.3

of three evaporitic horizons (Vergés *et al*., 1992), including Beuda Fm., Cardona Salt unit and Barbastro Fm. (Fig. 2C). These three horizons constitute the basal detachment of the triangle zone, where wide flats develop in the evaporitic formations (Vergés *et al*., 1992; Sans and Vergés, 1995).

RESULTS

AMS results from sites SLM1, SLM3, SLM8, SLM10, LC and LD (Fig. 3) including magnetic mineralogy and magnetic fabrics, are discussed in detail in Carrigan *et al*. (2016). Essentially, the Busa syncline and associated North and South limbs, reveal Type II and IIb magnetic fabrics. AMS data reveal a rather persistent subhorizontal, ESE-WNW trending magnetic lineation parallel to bedding strike (Fig. 3C), and mostly oblate magnetic ellipsoids with an anisotropy degree typically lower than 6%. Site SLM1 is located further South of the Busa syncline, on gently northwest-dipping strata, and still shows magnetic lineation trending ENE-WSW, parallel to the fold axis. In the majority of sites, principal axes of minimum

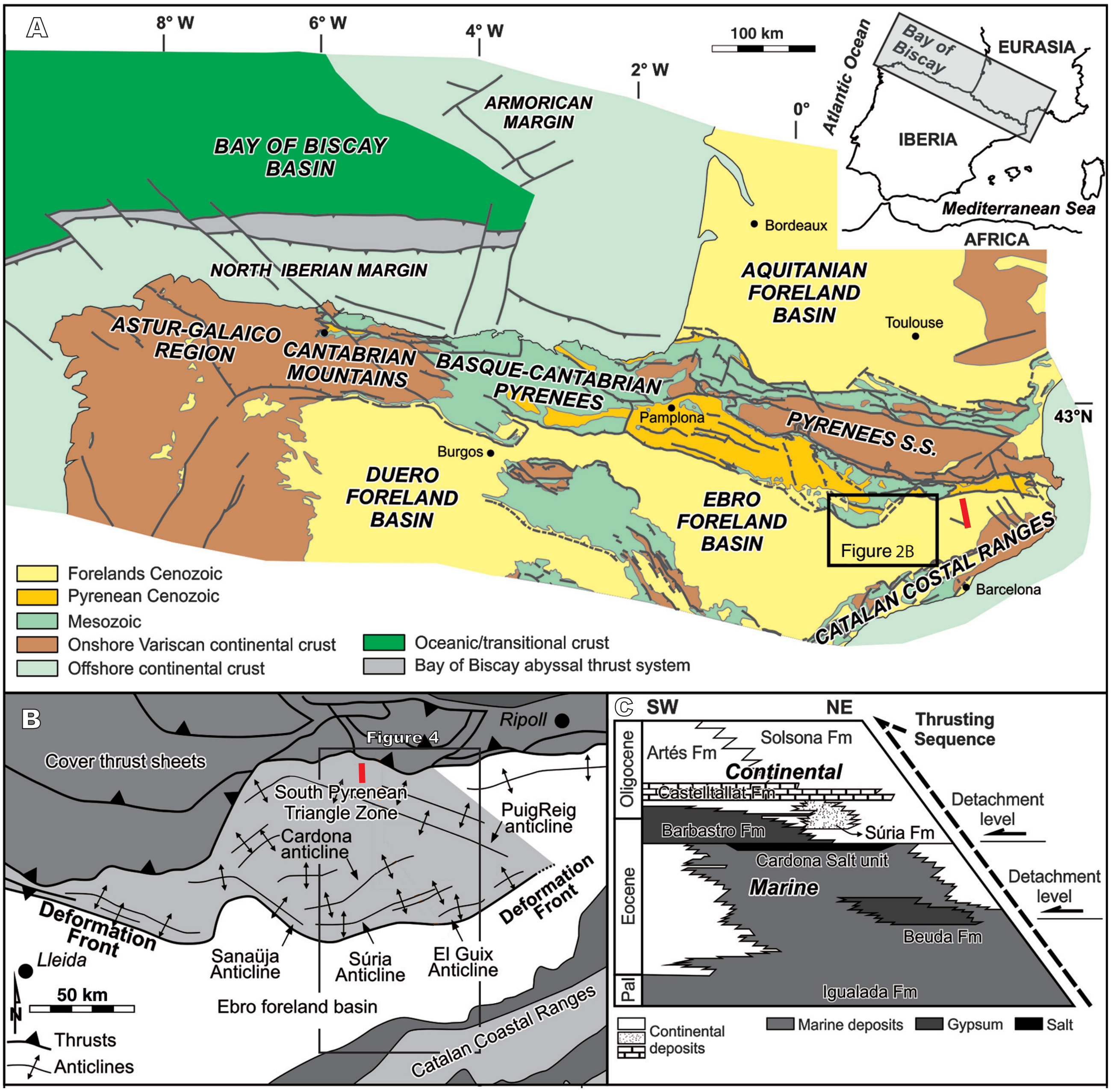

FIGURE 2. A) Geological setting of the study area in the Pyrenean fold and thrust belt. Red bar denotes "Ter-Freser section" (see text) B) Detailed geologic map with major folds and deformation front in the Eastern Pyrenees with the location of the Figure 4A. Red bar denotes location of the cross- section of Figure 3A. C) Synthetic stratigraphy showing the main formations including detachment levels in the study area (re-draw from Carola *et al.*, 2017).

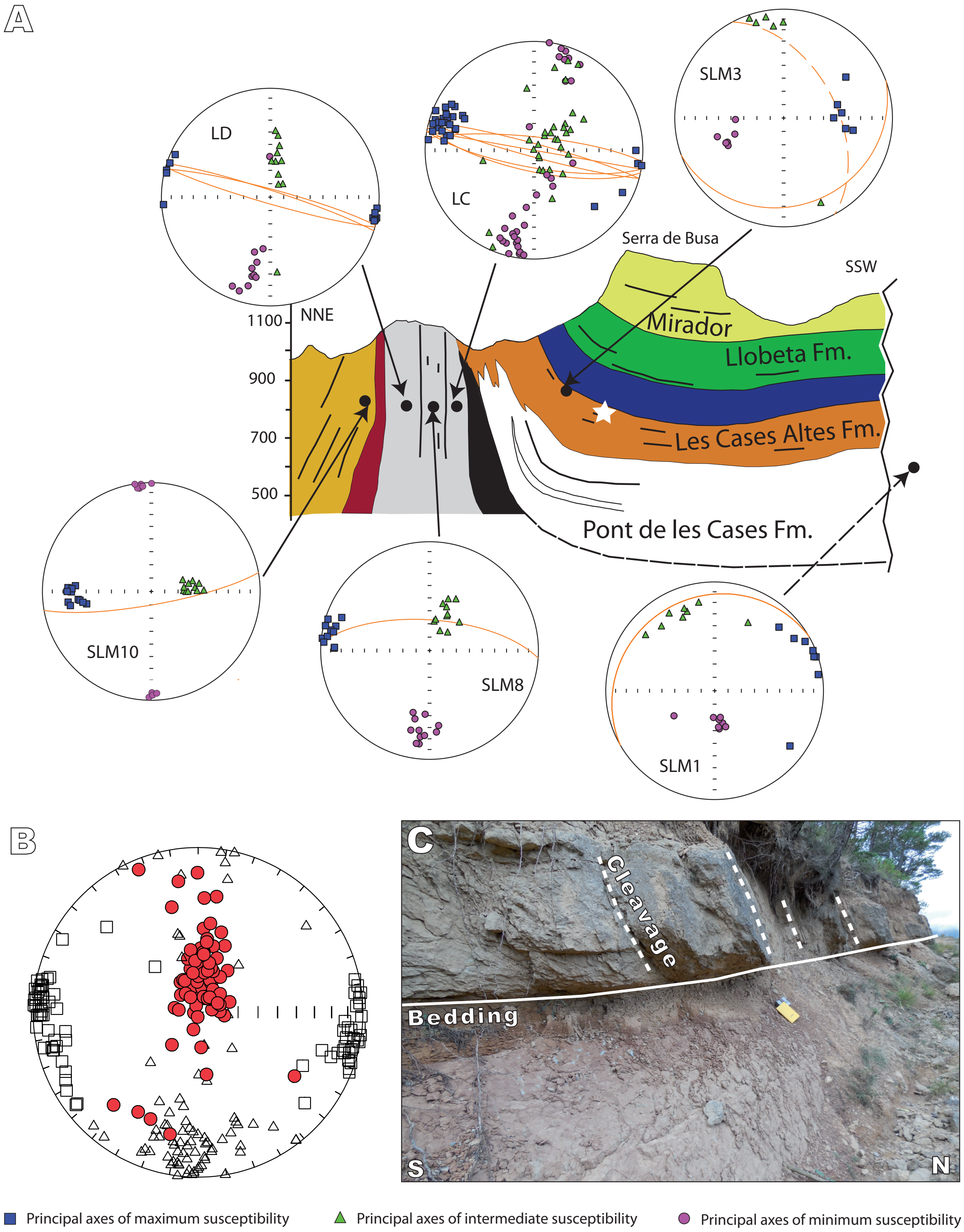

FIGURE 3. A) Profile through the western scarp of Serra de Busa viewed toward the East showing the main stratigraphic units and some representative Anisotropy of Magnetic Susceptibility (AMS) sites. Bedding is shown with a solid great-circle and cleavage with a dashed line great-circle. Star indicate approximate location of the picture in Figure 3C. AMS data reveal a rather persistent subhorizontal, ESE-WNW trending magnetic lineation parallel to bedding strike and dominantly oblate magnetic ellipsoids with an anisotropy degree typically lower than 6%. Site SLM1 is located further South, on gently North-dipping strata (modified from Carrigan *et al.*, 2016) (squares: K_{max}, triangles: K_{int}, dots: K_{min}). B) Principal axes of minimum susceptibility (K_{min}) typically plunge to the N after bedding correction in the northern limb of the syncline, which is consistent with layer parallel, top-to-North shear in the North limb. C) Photograph showing the spatial relationship between bedding (solid line) and cleavage (dashed line) in the field. Cleavage develops preferentially in the incompetent beds.

Geologica Acta, 16(4), 375-390 (2018)
DOI: 10.1344/GeologicaActa2018.16.4.3

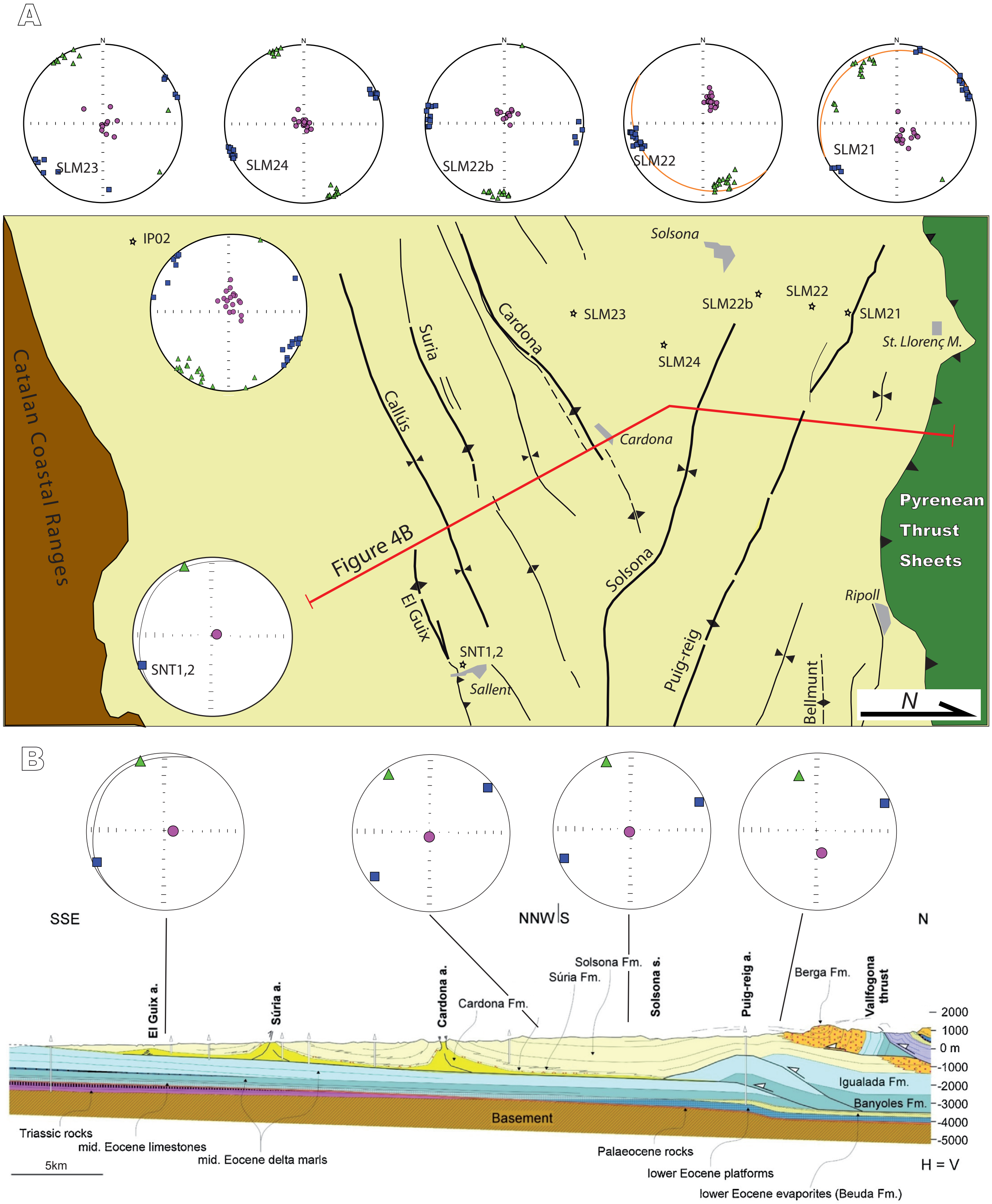

FIGURE 4. A) Location of the new study sites and results of the anisotropy of magnetic susceptibility (SNT1, SNT2 data modified from Sans *et al.*, 2003) South of the Busa syncline and along the Cardener Valley with location of the cross section of Figure 4B. Same symbols as in Figure 3C. B) Geological cross-section (modified from Vergés, 1993) including selected and simplified magnetic anisotropy results shown in A.

susceptibility (K_{min}) are slightly off from pole to bedding. This feature is more apparent when beds are restored to horizontal. Hence, K_{min} axes typically plunge to the North after bedding correction in the northern limb of the syncline. K_{min} axes distribution is consistent with layer parallel, top-to-North shear in the North limb. Such N-S shortening would post-date folding and is coherent with the observed microstructures such as spaced cleavage and small-scale shear zones. A Flinn diagram (Flinn, 1962) shows that the magnetic ellipsoids in the hinge of the fold are dominantly oblate and have higher degree of anisotropy (Carrigan *et al*., 2016). Cleavage is also quite pervasive in the hinge of the syncline which overall is suggestive of higher strain in that zone. These results are compatible with a limb rotation folding model and a pinned hinge zone (Ford *et al*., 1997; Carrigan *et al*., 2016). The tilt of the magnetic foliation poles (after bedding correction) also suggests shortening after folding, post-dating bedding-parallel shearing. Because AMS deformation occurs in incompletely lithified sediments that are being folded, AMS most likely was mostly accommodated by intergranular slip, leading to preferred grain orientation of phyllosilicates.

The new study sites are located further South of the Busa syncline and along the Cardener Valley (SLM21, SLM22, SLM22b, SLM23 and SLM24, see Table 1) (Fig. 4). In this area, the Solsona Fm. sandstones and siltstones record a Type IIa tectonic fabric (Fig. 4). All the localities that we have studied show K_{min} axes normal to bedding, whereas the K_{max} axes are grouped and striking around an ENE-WSW direction. Sites SLM21 and SLM22 reveal a slightly different pattern. These two sites are located on the South limb of the Puig-reig anticline, with a fold axis of WNW-ESE direction. The Puig-reig anticline is located on the footwall of the Vallfogona thrust (Vergés, 1993). AMS strain at both sites does not record the Puig-reig anticline trend, as they show a WSW-ENE trending magnetic lineation (Fig. 4). Site SLM22b, on the northern limb of the Solsona syncline, shows a well-developed magnetic lineation which conforms the orientation of the Solsona anticline (Fig. 4). Further South, site SLM24 displays a well-developed tectonic fabric, with a pronounced magnetic lineation that trends ENE-WSW, in flat-lying rocks. Last, site SLM23, although having somewhat higher axes dispersion, shows a similar orientation compared to the average magnetic lineation. The former site is located just few kilometers North of the Cardona anticline.

Overall, magnetic anisotropy factors (Pj and T) are similar to the values obtained by Carrigan *et al*. (2016) in the subhorizontal limb of the Busa syncline. It is worth pointing out are the results from site SLM22, on the southern limb of the Puig-reig anticline. At this locality K_{min} axes (Fig. 3B) are normal to bedding in the geographic reference frame and K_{max} axes cluster around a WSW direction (Fig. 4). Upon bedding correction, the magnetic lineation has a WSW-ESE, as bedding angle is only 20 degrees to the SW. It is somewhat surprising that the magnetic lineation in the southern limb of the Puig-reig and Solsona folds, which trend ~NW-SE, forms a high angle to the respective fold axes. The magnetic lineation is neither parallel to the bedding strike before bedding correction, which at first value could suggest that the magnetic lineation was first developed, by a NNW-SSE layer parallel shortening, and later folded by the Puig-reig anticline. We will return to this point in the next section.

We also consider the results of Sans *et al*. (2003) who report internal deformation in the Cenozoic units on the El Guix anticline (Fig. 4). This is a NE–SW trending fold detached above the Cardona salts that represents the frontal structure of the Pyrenean fold-and-thrust belt (Sans and Vergés, 1995). At all studied localities (Fig. 4) the magnetic lineation strikes between E-W to NE-SW, depending on the specific position within the complex structure. Two sites of that study (SNT1 and SNT2, Sans *et al*., 2003) on the northern limb of the anticline, show a well-developed magnetic lineation with a mean direction of ENE-WSW on beds that are sub-horizontal (Fig. 4). Such arrangement is interpreted as due to layer parallel shortening and is coherent with the orientation of the El Guix anticline axis (Sans *et al*., 2003).

TABLE 1. Anisotropy of magnetic susceptibility results. See site locations in Figure 4A. K_{max}, K_{int}, K_{min} are the principal susceptibilities. Dec: declination; Inc: Inclination; L: magnetic Lineation; F: magnetic Foliation; Pj: Anisotropy degree; T: Shape parameter

Site	K_{max}			K_{int}		K_{min}		Anisotropy Ratios and Parameters			
	N	Dec	Inc	Dec	Inc	Dec	Inc	L	F	Pj	T
SLM21	9	60.0	1.3	329.6	13.7	155.5	76.2	1.018	1.018	1.037	0.007
SLM22	18	259.0	12.9	164.2	19.8	20.0	66.0	1.013	1.015	1.029	0.079
SLM22b	13	276.6	1.9	186.3	9.3	18.0	80.5	1.015	1.043	1.061	0.472
SLM23	11	229.9	2.0	320.1	4.1	113.3	85.4	1.016	1.032	1.049	0.316
SLM24	15	66.8	0.1	156.8	1.5	334.0	88.5	1.019	1.039	1.060	0.350

Geologica Acta, 16(4), 375-390 (2018)
DOI: 10.1344/GeologicaActa2018.16.4.3

Last, we also include site IP02 in our study (Pascual and Parés, 1990), which is on flat-lying fine-grained sandstones and siltstones of upper Eocene age and which has sedimentary fabric. K_{max} axes conform a NW-SE trend, which is consistent with the observed paleocurrent directions (*e.g.* Anadón *et al.*, 1989). This locality is located about ~20km South of the Cardona anticline, is found on flat lying fine-grained sandstones and siltstones of Oligocene age.

DISCUSSION

Our new AMS data support and complement previous results by Carrigan *et al.* (2016) in the Busa syncline to the North of the study area (Fig. 3). The maximum axes of susceptibility (K_{max}) typically but not always reflect the intersection between horizontal shortening and bedding plane and record the progression of the ~N-S tectonic shortening towards the thrust front. Such magnetic lineation roughly keeps an E-W to ENE-WSW orientation, which is consistent with the kilometric-scale structure. In detail though, magnetic lineation experiences a change in orientation from North to South. The bulk of the magnetic ellipsoids in the North (Carrigan *et al.*, 2016) are coherent with the fault-related Busa fold, with K_{max} axes ~E-W trending, *i.e.* parallel to the fold axis, and the K_{min} either normal to bedding or describing a N-S girdle. Nevertheless, few kilometers South of the Busa syncline, sites SLM21 and SLM22 reveal a different pattern, as they do not conform the Puig-reig anticline fold axis. The Cardona anticline trends NE-SW and is a South-verging detachment fold developed where the Cardona Fm. salt is thickest. Given the coincidence between the orientation of the Cardona fold axis and site SLM23 magnetic lineation, it is plausible that this site records the shortening related to the anticline. Otherwise, sites located North of the Cardona anticline, disagree with the structural data, in that magnetic lineation is oblique to the main structures: K_{max} in sites SLM21 and SLM22, between Puig-reig anticline and the Solsona syncline, form an acute angle with the Puig-reig anticline. Nevertheless, few kilometer South at locality SLM24, on the South limb of the Solsona syncline, K_{max} forms an acute angle with its fold axis and is rather parallel to the next major structure, the Cardona anticline. Both folds, Puig-reig and Solsona, are major structures in the eastern Pyrenees. In fact, Sans *et al.* (1996) distinguish two regions in this area according to the folding and thrusting orientation: A northeastern region with ESE-WNW trending structures (*e.g.* Puig-reig anticline, Solsona syncline), and a central region with NE-SW trending structures (*e.g.* Cardona, Suria, El Guix folds) (Fig. 2A), owing to the pinch-outs of the evaporitic horizons. In this scenario, the Puig-reig anticline represents the surface structure of the ramp of the northern thrust wedge that is located at the southern pinch-out of the Beuda Fm. (Fig. 2C) (Vergés, 1993; Sans *et al.*, 1996). On the other hand, the NE-SW Cardona anticline develops where the homonymous formation is thickest (aprox. 300m) and where the basal slope of the Cardona Fm. is almost horizontal (Vergés *et al.*, 1992). Anticlines such El Guix and Súria are related to the southern pinch-out of the Cardona salt.

Taken at first value, the bulk of the magnetic data suggests that PES dissipates few kilometers South of the Callús syncline (Fig. 4), the southernmost deformation front in the studied sector, so somewhere North of site IP02, which records a sedimentary fabric. Such observation somewhat contrasts with existing magnetic fabric results East and West of the studied sector. NW of Zaragoza, Pueyo-Anchuela *et al.* (2010) report a tectonic magnetic fabric in flat-lying sediments several tens of kilometers South of the deformation front ("Sos section" of Pueyo-Anchuela *et al.*, 2010; Teletzke *et al.*, 2011; Teletzke, 2012) (Fig. 5). Similar results were reported by Soto *et al.* (2009), in Miocene sediments NW and NE of Zaragoza, which show WNW-ESE trending K_{max} axes which are normal to the main tectonic shortening. On the other hand, in the NE of the Ebro foreland Basin, Parés *et al.* (1999) reported penetrative strain in the flat-lying marls of the Igualada Fm., in localities that are South of the Bellmunt anticline, the southernmost expression of tectonic shortening at the surface (Ter-Freser section, Fig. 2B). The corollary of all these results from the Ebro foreland Basin are that localities as far as 60km from the deformation front show penetrative strain according to the magnetic fabric data that is consistent with Pyrenean shortening directions. Nevertheless, our own study along the Cardener valley (South of Busa) suggests that PES, as recorded in the magnetic fabrics, is absent at a distance not longer than ~20km from the southernmost fold. The distance between observed PES and the deformation front changes along strike as it varies from ~20 to ~60km. What we observe in the Pyrenean foreland Basin is that shortening is revealed by the magnetic fabrics in areas relatively far away from the frontal fold. The lateral (N to S) extent of PES in the sedimentary cover should reflect the strain propagation in these areas, so it is possible that differences in the strength of the basal décollment level that allows strain propagation determines the development and extent of PES. In the northeastern region (Ter-Freser), the southernmost contractional structure (Bellmunt anticline, Fig. 4) is located above the Beuda Fm. The Beuda thrust-front has as a main detachment level sediments consisting of shales, gypsum and some salt (Sans, 2003). In the central region, where Cardona, Solsona, etc folds are found, the detachment is the Cardona Fm., which consists of anhydrite massive halite and potassium salt (Pueyo, 1975). Further West, in the West-Central Pyrenees (Sos section), the Peña flexure is the southernmost expression of deformation. Although

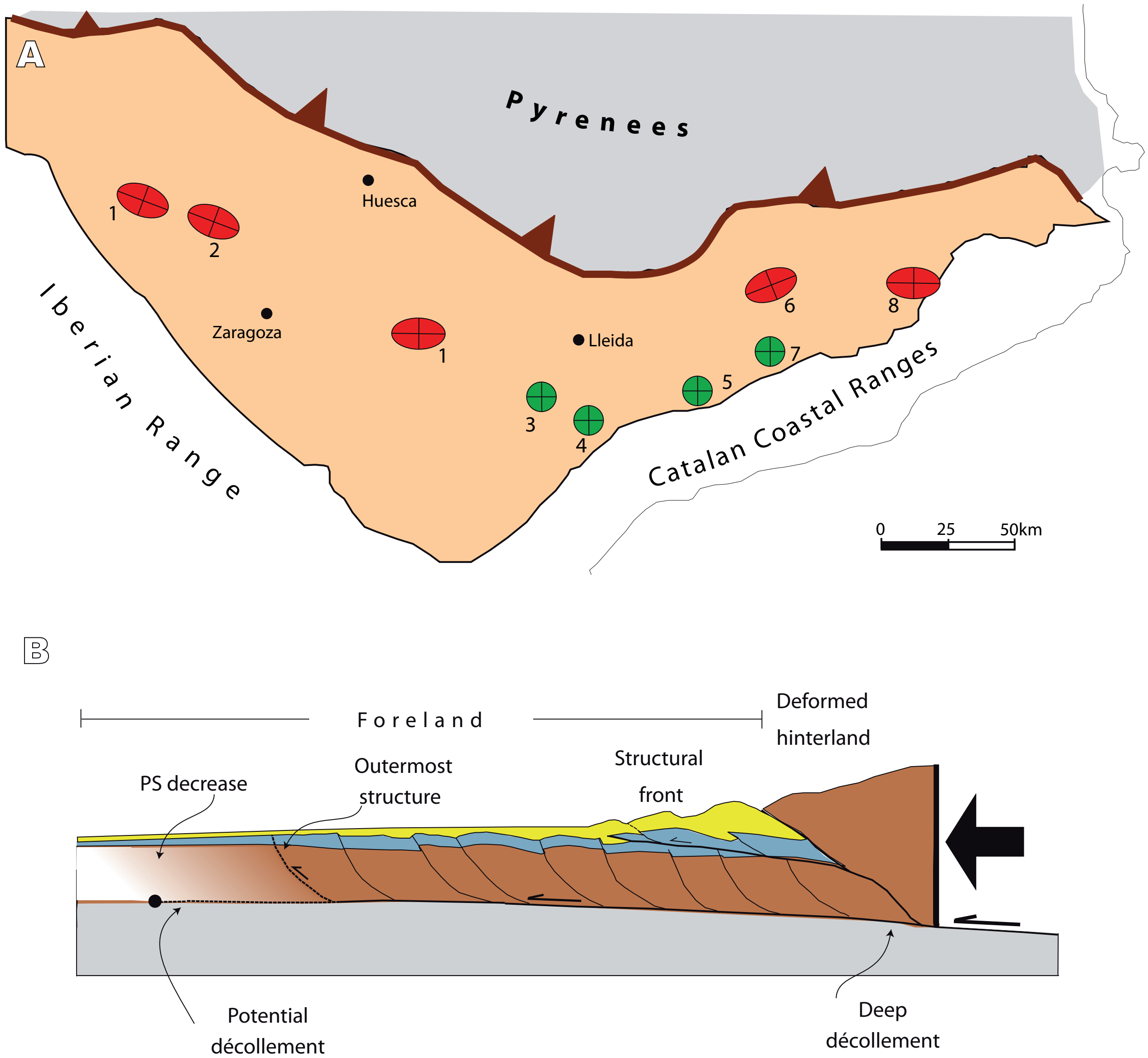

FIGURE 5. A) Sketch of the Ebro foreland Basin, including the areas where penetrative strain has been established with anisotropy of magnetic susceptibility. Ellipses represent the Y/Z plane of the strain ellipsoid. 1: Soto *et al.* (2009); 2: Pueyo-Anchuela *et al.* (2010); 3: Gomis (1997); 4 and 5: Barberà (1999); 6: Sans *et al.* (2003); 7: Pascual and Parés (1990); 8: Parés *et al.* (1999). B) Conceptual cross section (not to scale) across an imbricated thrust wedge, showing the extent of the Penetrative Strain (PES) forelandward away from the structural front, in relation to the outermost structure (modified from Lacombe and Mouthereau, 1999).

this structure has been interpreted as a décollement fold cored by Triassic evaporites (Oliva-Urcia *et al.*, 2016), it could alternatively represent an antiformal stack. Be that as it may, a deeper detachment in the region is thought to be found in the Keuper facies (clays and gypsum) (Teixell, 1996; Oliva-Urcia *et al.*, 2012, 2016). Hence, whereas the detachment level includes gypsum-rich formations in the NE and W sectors, salt is more abundant in the central sector. A consequence of the variation in the detachment level rheology within the basin is that in the Cardener-Solsona area the sedimentary cover is deformed on a very incompetent detachment, the Cardona Fm. On the contrary, in both NE sector (Ter-Freser) and West-Central Pyrenees (Sos section), sedimentary cover is shortened on a still weak but more competent detachment layer (Triassic and Paleogene clays and gypsum).

Rheology of the detachment has a strong influence on the PES of the hangingwall rock units (*e.g.* Aubourg *et al.*, 2004; Robion *et al.*, 2007; Nilforoushan *et al.*, 2008). For example, Nilforoushan *et al.* (2008) developed sandbox models of fold-thrust belts and accretionary prisms and results show a clear correlation between décollement basal friction on surface and volumetric strain in the models. It appears that high-friction décollements promote PES in the cover. If extrapolated to nature, the results indicate that PES is expected to be greater in fold-thrust belts shortened above stiffer décollements than in areas that were shortened above a weaker décollement. Robion *et al.* (2007) and Aubourg *et al.* (2010) have also noticed that the efficiency of the detachment seems to determine the magnetic fabric in the sedimentary cover. Hence, according to their results, when stronger (stiffer) layers such as gypsum dominate in the detachment, strain develops further out into the foreland, whereas when more efficient rocks such as salt dominate, then strain is confined closer to the thrust front. Although the balance between orogenic wedges to décollement strength is critical, it follows that friction often determines the PES that is observed in the sedimentary cover, even though strain develops mostly by linear viscous deformation. Hence, where friction is high the tendency is that sediments develop a layer parallel shortening fabric Type IIb or even Type III (Fig. 1), whereas when the detachment is more efficient and the friction is lower, a Type IIa develops and is preserved in the sediments. Sans (2003) used analogue models to document how the rheology of the detachment horizons controls the deformation front in the eastern Pyrenees. In that experiment very ductile detachments promote folding, whereas when detachment is less ductile (higher friction) thrusting is the dominant deformation mechanism, in agreement with natural examples as in the Rockies (Anastasio *et al.*, 1997). In natural examples real examples, in a similar way, localized lower efficiency detachment in the South Pyrenean foreland Basin could possibly promote a further extent forelandwards of penetrative strain as seen by the magnetic fabrics.

The control that the detachment strength exerts onto the strain in the sedimentary cover has been noticed for years in several fold and thrust belts. For example, in the Central Appalachians large wavelength detachment folds occur underlain by Silurian evaporates, whereas in the Southern Appalachians thrust faults dominate (Gwinn, 1964; Davis and Engelder, 1985; Hatcher *et al.*, 1989). In the Northern Canadian Rockies folding dominates in areas where thick evaporate levels are found (*e.g.* Thompson, 1981), whereas to the South thrusting is more abundant (*e.g.* Price and Mountjoy, 1970).

CONCLUSIONS

Both Berga and Solsona formations, in the Eastern Pyrenees, display magnetic fabric ellipsoids whose axes orientation can be taken as a proxy for internal deformation. Deformation occurred as layer parallel shortening ahead of the Pyrenean thrust sheets (Vallfogona Thrust). The magnetic lineation, as defined by the grouping of Kmax axes, is generally consistent with thrust and fold axes that have an ENE-WSW orientation, and not the set of NW-SE trending structures that are also prominent in the Eastern Pyrenees. Although several other options are possible, a two stage-deformation, with a slight change of the maximum shortening direction is a possible mechanism. In the Busa area, the appearance of cleavage that is not strictly axial planar to the Busa fold might suggest that there is a time lag between the onset of folding and the development of cleavage, or that folding developed within a transpressive regime (Ford *et al.*, 1997).

Both in the easternmost part of the Ebro foreland Basin (Ter-Freser transect), and in the western-Central Pyrenees (Sos section), penetrative deformation, as revealed by the magnetic fabrics, extents much farther South than in the eastern region (Cardoner transect). The possible role of both the Iberian Range and the Catalan Coastal Ranges as a buttress effect on the PES needs to be further explored. We acknowledge that more observations are necessary to determine the location of the southernmost sediments having PES, and what minimum differential stress level is necessary to produce a tectonic fabric in the AMS but a possible explanation resides in the effectiveness of the detachment levels. When stronger layers dominate in the detachment (*e.g.* Keuper facies), penetrative strain seems to reach larger distances into the foreland, whereas when the detachment is mostly due to salt (*e.g.* Cardona Fm.), then internal strain seems to dissipate closer to the deformation front. Such hypotheses need to be further tested with additional AMS fabric studies in particular along the southern margin of the Ebro foreland Basin.

ACKNOWLEDGMENTS

We thank the reviewers (Charles Aubourg and anonymous) and the editors (Josep M. Casas and Eduard Roca) for their helpful constructive comments and suggestions. Josep M. Parés would like to thank his former advisor Prof. Pere Santanach for all the enjoyable and fruitful days in the field, and the guidance that he gave him over the early stage of his career. Research partially funded by Ministerio de Economía, Industria y Competitividad (MINECO) Grant CGL2014-62296-EXP to JMP.

REFERENCES

Alonso, J.L., Colombo, F., Riba, O., 2011. Folding mechanisms in a fault-propagation fold inferred from analysis of unconformity angles: The Sant Llorenç growth structure (Pyrenees, Spain). In: McClay, K., Shaw, J., Suppe, J. (eds.). Thrust fault-related folding, American Association of Petroleum Geologists Memoir, 94, 137-151.

Anadón, P., Cabrera, L., Colldeforns, B., Saez, A., 1989. Los sistemas lacustres del Eoceno superior y Oligoceno del sector oriental de la Cuenca del Ebro. Acta Geologica Hispanica, 24, 205-230.

Anastasio, D., Parés, J.M., Kodama, K., Troy, J., Pueyo, E., 2015. Anisotropy of Magnetic Susceptibility (AMS) records synsedimentary deformation kinematics at Pico del Aguila anticline, Pyrenees, Spain. In: Pueyo, E., Cifelli, F., Sussman, A.J., Oliva-Urcia, B. (eds.). Palaeomagnetism in Fold and Thrust Belts: New Perspectives. Geological Society of London, 425 (Special Publications), 129-144. DOI: 10.1144/SP425.8

Aubourg, C., Rochette, P., Vialon, P., 1991. Subtle stretching lineation revealed by magnetic fabric of Callovian-Oxfordian black shales (French Alpes). Tectonophysics, 185, 211-223.

Aubourg, C., Smith, B., Bakhtari, H., Guya, N., Eshragi, A., Lallemant, S., Molinaro, M., Braud, X., Delauny, S., 2004. Post-Miocene shortening pictured by magnetic fabric across the Zagros-akran syntaxis, Iran. In: Sussman, A.J., Weil, A.B. (eds.). Orogenic Curvature: Integrating aleomagnetic and Structural Analyses. Geological Society of America, 383 (Special Paper), 17-40.

Aubourg, C., Smith, B., Eshraghi, A., Lacombe, O., Authemayou, C., Amrouch, K., Bellier, O., Mouthereau, F., 2010. New magnetic fabric data and their comparison with palaeostress markers in the Western Fars Arc (Zagros, Iran): tectonic implications. Geological Society of London, 330 (Special Publications), 97-120.

Averbuch, O., Frizon de Lamotte, D., Kissel, C., 1992. Magnetic fabric as a structural indicator of the deformation path within a fold thrust structure: a test case from the Corbieres (NE Pyrenees, France). Journal of Structural Geology, 14, 461-474.

Bakhtari, H.R., de Lamotte, D.F., Aubourg, C., Hassanzadeh, J., 1998. Magnetic fabrics of tertiary sandstones from the Arc of Fars (Eastern Zagros, Iran). Tectonophysics, 284, 299-316.

Balsley, J.R., Buddington, A.F., 1960. Magnetic susceptibility and fabric of some Adirondack granites and orthogneisses. American Journal of Science, 258, 6-20.

Barberà, X., 1999. Magnetoestratigrafia del Oligocè del sector sud-oriental de la Conca del Ebre: implicacions magnetocronològiques i sequencials. PhD Thesis. Barcelona, University of Barcelona, 337pp.

Barrier, L., Proust, J.N., Nalpas, T., Robin, C., Guillocheau, F., 2010. Control of Alluvial Sedimentation at Foreland-Basin Active Margins: A Case Study from the Northeastern Ebro Basin (Southeastern Pyrenees, Spain). International Journal of Sediment Research, 80, 728-749.

Borradaile, G.J., Tarling, D.H., 1981. The influence of deformation mechanisms on magnetic fabrics in weakly deformed rocks. Tectonophysics, 77, 151-168.

Borradaile, G.J., Jackson, M., 2004. Anisotropy of magnetic susceptibility (AMS): magnetic petrofabrics of deformed rocks. In: Martin-Hernandez, F., Lüneburg, C.M., Aubourg, C., Jackson, M. (eds.). Magnetic Fabrics: Methods and Applications, Geological Society of London, 238 (Special Publications), 299-360.

Burberry, C.M., 2015. Spatial and temporal variation in penetrative strain during compression: insights from analog models. Lithosphere, 7, 611-624. DOI: 10.1130/L454.1

Carola, E., Ferrer, O., Vidal-Royo, O., Muñoz, J.A., 2017. Interpretation of salt-cored frontal structures in the Southern Pyrenees guided by analog modeling, surface and subsurface data. Interpretation, 5(1), SD39-SD54. DOI: 10.1190/INT-2016-0093.1

Carrigan, J., Anastasio, D., Kodama, K., Parés, J.M., 2016. Fault-related fold kinematics recorded by terrestrial growth strata, Sant Llorenç de Morunys, Pyrenees Mountains, NE Spain. Journal of Structural Geology, 91, 161-176.

Clark, B.R., 1970. Mechanical formation of preferred orientation in clays. American Journal of Science, 269, 250-266.

Collombat, H., Rochette, P., Vialon, P., 1995. Magnetic fabric as a strain indicator in unconsolidated sediments of the Chile Triple Junction area. In: Lewis, S.D., Behrmann, J.H., Musgrave, R.J., Cande, S.C. (eds.). Proceedings of the Ocean Drilling Program, Scientific Results, 141, College Station, TX (Ocean Drilling Program), 29-49.

Cooper, M.A., Garton, M.R., Hossack, J.R., 1983. The origin of the Basse Normandie duplex, Boulonnais, France. Journal of Structural Geology, 5(2), 139-152.

Craddock, J.P., 1992. Transpression during tectonic evolution of the Idaho-Wyoming fold-and- thrust belt. In: Link, P.K., Kuntz, M.A., Platt, L.B. (eds.). Regional Geology of Eastern Idaho and Western Wyoming. Geological Society of America Memoir, 179, 55-81.

Crosby, G.W., 1969. Radial movements in the western Wyoming salient of the Cordilleran overthrust belt. Geological Society of America Bulletin, 80(6), 1061-1078.

Davis, D.M., Engelder, T., 1985. The role of salt in fold-and-thrust belts. Tectonophysics, 119, 67-88.

Debacker, T.N., Robion, P, Sintubin, M., 2004. The anisotropy of magnetic susceptibility (AMS) in low-grade, cleaved pelitic rocks: influence of cleavage/bedding angle and type and relative orientation of magnetic carriers. In: Martin-Hernandez, F., Lüneburg, C.M., Aubourg, C., Jackson, M. (eds.). Magnetic Fabrics: Methods and Applications. Geological Society of London, 238 (Special Publications), 77-107.

Engelder, T., 1979. The nature of deformation within the outer limits of the central Appalachian foreland fold and thrust belt in New York State. Tectonophysics, 55, 289-310.

Engelder, T., Engelder, R., 1977. Fossil distortion and decollement tectonics of the Appalachian Plateau. Geology, 5, 457-460.

Evans, M.A., Dunne, W.M., 1991. Strain factorization and partitioning in the North Mountain thrust sheet, central Appalachians, USA. Journal of Structural Geology, 13, 21-35.

Faill, R.T., Nickelsen, R.P., 1999. Appalachian mountain section of the Valley and Ridge province. In: Schultz, C.H. (ed.). The Geology of Pennsylvania. Pennsylvania Geological Survey, 1 (Special Publication), 268-285.

Geologica Acta, 16(4), 375-390 (2018)
DOI: 10.1344/GeologicaActa2018.16.4.3

Fellows, R.E., 1943. Recrystallization and flowage in Appalachian quartzite. Bulletin of the Geological Society of America, 54, 1399-1432.

Fernández, A., 1987. Preferred orientation developed by rigid markers in two-dimensional simple shear strain: A theoretical abd experimental study. Tectonophysics, 136, 151-158.

Flinn, D., 1962. On folding during three-dimensional progressive deformation. Quarterly Journal of the Geological Society of London, 118, 385-428.

Fourmarier, P., 1923. De l'importance de la Charge dans le developpement du Clivage schisteux. Bulletins de l'Académie royal Des Sciences, des lettres et des beaux-arts de Belgique, Classe des sciences sciences et belles-lettres de Bruxelles, 5, 454.

Ford, M., Williams, E.A., Artoni, A., Vergés, J., Hardy, S., 1997. Progressive evolution of a fault-related fold pair from growth strata geometries, Sant Llorenç de Morunys, SE Pyrenees. Journal of Structural Geology, 19, 413-634.

Frizon de Lamotte, D., Souqué, C., Grelaud, S., Robio, P., 2002. Early record of tectonic magnetic fabric during inversión of a sedimentary basin. Short review and examples from the Corbières transfer zone (France). Bulletin de la Société géologique de France, 173, 461-469.

Geiser, P.A., 1988. Mechanisms of thrust propagation: some examples and implications for the analysis of overthrust terranes. Journal of Structural Geology, 10, 829-845.

Gil-Imaz, A., Pocoví, A., Lago San José, M., Parés, J.M., 2000. Effect of lithostatic pressure and tectonic deformation on the magnetic fabric (anisotropy of magnetic susceptibility) in low-grade metamorphic rocks. Journal of Geophysical Research, 105, 21.305-21.317.

Gomis, E., 1997. Precisión sobre la magnetoestratigrafía de las sucesiones dl Oligoceno Superior-Mioceno inferior en los valles del Cinca, Segre y Ebro (Sector SE de la cuenca del Ebro, provincias de Lleida, Zaragoza y Huesca). M.Sc. Thesis. Barcelona, Universitat de Barcelona, 104pp.

Gwinn, V.E., 1964. Thin-skinned tectonics in the Plateau and northwestern Valley and Ridge provinces of the central Appalachians. Geological Society of America Bulletin, 75, 863-900.

Hatcher, R.D., Jr., Thomas, W.A., Geiser, P.A., Snoke, A.W., Mosher, S., Wiltschko, D.V., 1989. "Alleghanian orogen". In: Hatcher, R.D., Thomas, W.A.Jr., Viele, G.W. (eds.). The Appalachian-Ouachita orogen in the United States. Geological Society of America (GSA), Boulder, 233-318.

Hirt, A.M., Lowrie, W., Lüneburg, C., Lebit, H., Engelder, T., 2004. Magnetic and mineral fabric development in the Ordovician Martinsburg Formation in the Central Appalachian Fold and Thrust Belt, Pennsylvania. In: Martin-Hernandez, F., Lüneburg, C.M., Aubourg, C., Jackson, M. (eds.). Magnetic Fabrics: Methods and Applications. Geological Society of London, 238 (Special Publications), 109-126.

Holl, J.E., Anastasio, D.J., 1995. Cleavage development within a foreland fold and thrust belt, southern Pyrenees, Spain. Journal Structural Geology, 17, 357-369.

Homza, T.X., Wallace, W.K., 1997. Detachment folds with fixed hinges and variable detachment depth, northeastern Brooks Range, Alaska. Journal of Structural Geology, 19, 337-354.

Hossack, J.R., 1978. The correction of stratigraphic sections for tectonic finite strain in the Bygdin area, Norway. Journal of the Geological Society, 135, 229-241.

Jelinek, V., 1978. Statistical processing of anisotropy of magnetic susceptibility measured on groups of specimens. Studia Geophysica et Geodaetica, 22, 50-62.

Jelinek, V., 1981. Characterization of the magnetic fabrics of rocks. Tectonophysics, 79, T63-T67.

Kanamatsu, T., Parés, J.M., Kitamura, Y., 2012. Pliocene shortening direction of Nankai Trough off Kumano southwest Japan, Sites IODP C0001 and C0002, Expedition 315, anisotropy of magnetic susceptibility analysis for paleostress. Geochemistry Geophysics Geosystems, 13, Q0AD22. DOI: 10.1029/2011GC003782

Kissel, C., Barrier, E., Laj, C., Lee, T.Q., 1986. Magnetic fabric in 'undeformed' marine clays from compressional zones. Tectonics, 5, 769-781.

Kodama, K.P., Sun, W.W., 1992. Magnetic Anisotropy as a Correction for Compaction-caused Paleomagnetic Inclination Shallowing. Geophysical Journal International, 111, 465-469.

Koyi, H.A., Sans, M., Teixell, A., Cotton, J., Zeyen, H., 2004. The significance of penetrative strain in the restoration of shortened layers—insights from sand models and the Spanish Pyrenees. Thrust, tectonics and hydrocarbon systems, American Association of Petroleum Geologists Memoir, 82, 207-222.

Lacombe, O., Mouthereau, F., 1999. What is the real front of orogens? The Pyrenean orogen case. Comptes Rendus de l'Académie des Sciences, 329(II), 889-896.

Larrasoaña, J.C., Pueyo, E.L., Parés, J.M., 2004. An integrated AMS, structural, palaeo- and rockmagnetic study of the Eocene marine marls from the Jaca-Pamplona basin (Pyrenees, N Spain): new insights into the timing of magnetic fabric acquisition in weakly deformed mudrocks. In: Martin-Hernandez, F., Lüneburg, C.M., Aubourg, C., Jackson, M. (eds.). Magnetic Fabrics: Methods and Applications. The Geological Society of London, 238 (Special Publications), 127-144.

Lüneburg, C.M., Lampert, S.A., Lebit, H.D., Hirt, A.M., Casey, M., Lowrie, W., 1999. Magnetic anisotropy, rock fabrics and finite strain in deformed sediments of SW Sardinia (Italy). Tectonophysics, 307, 51-74.

McNaught, M.A., Mitra, G., 1996, The use of finite strain data in constructing a retrodeformable cross-section of the Meade thrust sheet, southeastern Idaho, U.S.A. Journal of Structural Geology, 18, 573-583.

Martín-Hernández, F., Hirt, A.M., 2001. Separation of ferrimagnetic and paramagnetic anisotropies using a high-field torsion magnetometer. Tectonophysics, 337, 209-221.

Mitra, S., 1990. Fault propagation folds: Geometry, kinematic evolution and hydrocarbon traps. American Association of Petroleum Geologists Memoir, 74, 921- 945.

Mitra, G., 1994. Strain variation in thrust sheets across the Sevier fold-and-thrust belt (Idaho-Utah-Wyoming): implications for section restoration and wedge taper evolution. Journal of Structural Geology, 6, 51-61.

Mochales, T., Pueyo, E.L., Casas, A.M., Barnolas, A., Oliva-Urcia, B., 2010. Anisotropic magnetic susceptibility record of the kinematics of the Boltaña Anticline (Southern Pyrenees). Geological Journal, 45, 562-581.

Mukul, M., Mitra, G., 1998. Finite strain and strain variation analysis in the Sheeprock Thrust Sheet: an internal thrust sheet in the Provo salient of the Sevier Fold-and-Thrust belt, Central Utah. Journal of Structural Geology, 20, 385-405.

Nagata, T., 1961. Rock magnetism. 2nd edition, Maruzen (Tokyo), 350pp.

Nickelsen, R.P., 1983. Aspects of Alleghanian deformation. In: Nickelsen, R.P., Cotter, E., (eds.). Silurian Depositional History and Alleghanian Deformation in the Pennsylvania Valley and Ridge. Field Conference of Pennsylvania Geologists 49th Annual, Danville, Guidebook, 29-39.

Nilforoushan, F., Koyi, H.A., Swantesson, J.O.H., Talbot, C.J., 2008. Effect of basal friction on surface and volumetric strain in models of convergent settings measured by laser scanner. Journal of Structural Geology, 30, 366-379.

Nye, J.F., 1957. The Physical Properties of Crystals. Oxford, Clarendon Press, 322pp.

Oliva-Urcia, B., Larrasoaña, J.C., Pueyo, E.L., Gil-Imaz, A., Mata, P., Parés, J.M., Schleicher, A., 2009. Disentangling magnetic subfabrics and their link to deformation processes in cleaved sedimentary rocks from the Internal Sierras (west central Pyrenees, Spain). Journal of Structural Geology, 31, 163-176.

Oliva-Urcia, B., Casas, A.M., Pueyo, E.L., Pocoví-Juan, A., 2012. Structural and paleomagnetic evidence for non-rotational kinematics of the South Pyrenean Frontal Thrust at the western termination of the External Sierras (southwestern central Pyrenees). Geologica Acta, 10(2), 125-144.

Oliva-Urcia, B., Beamud, E., Garcés, M., Arenas, C., Soto, R., Pueyo, E., Pardo, G., 2016. New magnetostratigraphic dating of the Paleogene syntectonic sediments of the West-Central Pyrenees: Tectonostratigraphic implications. In: Pueyo, E.L., Cifelli, F., Sussman, A.J., Oliva-Urcia, B. (eds.). Palaeomagnetism in Fold and Thrust Belts: New Perspectives. The Geological Society of London, 425 (Special Publications), 107-128. DOI: 10.1144/SP425.5

Owens, W., 1993. Magnetic fabric studies of samples from Hole 808C, Nankai Trough. In: Hill, I.A., *et al*. (eds.). Proceedings of the Ocean Drilling Program. Science Results, 131, Ocean Drilling Program, College Station, TX, 301-310. DOI: 10.2973/odp.proc.sr.131.130.1993

Parés, J.M., 2015. Sixty Years of Anisotropy of Magnetic Susceptibility in deformed sedimentary rocks. Frontiers of Earth Science, 3(4), 1-13. DOI: 10.3389/feart.2015.00004

Parés, J.M., Dinarès-Turell, J., 1993. Magnetic fabric in two sedimentary rock types from the Southern Pyrenees. Journal of Geomagnetism and Geoelectricity, 45, 193-205.

Parés, J.M., van der Pluijm, B., Dinarés-Turell, J., 1999. Evolution of magnetic fabrics during incipient deformation of mudrocks (Pyrenees, northern Spain). Tectonophysics, 307, 1-14.

Parés, J.M., van der Pluijm, B.A., 2003. Magnetic fabrics in low-strain mudrocks: AMS of pencil structures in the Knobs Formation, Valley and Ridge Province, US Appalachians. Journal of Structural Geology, 25, 1349-1358.

Parés, J.M., Carrigan, J., Anastasio, D., Kodama, K., 2016. Rock magnetic and reversal stratigraphy in terrestrial deposits: Recovering fault slip rates in growth strata. IX Congreso geológico de España. Huelva, 2016, 234.

Pascual, O., Parés, J.M., 1990. Estudio preliminar de los materiales comprendidos en el tránsito Eoceno-Oligoceno en el borde SE de la Cuenca del Ebro. Revista de la Sociedad Geológica de España, 3, 323-333.

Price, R.A., Mountjoy, E.W., 1970. Geologic structure of the Canadian Rocky Mountains between Bow and Athabasca Rivers-a progress report. Geological Association of Canada, 6 (Special Paper), 7-25.

Pueyo, J.J., 1975. Estudio petrológico y geoquímico de los yacimientos potásicos de Cardona, Súria, Sallent (Barcelona, España). PhD Thesis. Barcelona, Universitat de Barcelona, 300pp.

Pueyo-Anchuela, O., Pocoví A., Gil Imaz, A., 2010. Tectonic imprint in magnetic fabrics in foreland basins: a case study from the Ebro Basin, N Spain. Tectonophysics, 492, 150-163.

Puigdefàbregas, C., Muñoz, J.A., Marzo, M., 1986. Thrust Belt Development in the Eastern Pyrenees and Related Depositional Sequences in the Southern Foreland Basin. In: Allen, P.A., Homewood, P. (eds.). Foreland Basins. Oxford (UK), Blackwell Publishing Ltd., 229-246.

Puigdefàbregas, C., Muñoz, J.A., Vergés, J., 1992. Thrusting and foreland basin evolution in the Southern Pyrenees. In: McClay, K.R. (ed.). Thrust Tectonics. Dordrecht, Springer, 247-254. DOI: 10.1007/978-94-011-3066-09

Riba, O., 1973. Las discordancias sintectónicas del Alto Cardener (Prepirineo Catalán), ensayo de interpretación evolutiva. Acta Geológica Hispánica, 8, 90-99.

Riba, O., 1976. Syntectonic unconformities of the Alto Cardener, Spainish Pyrenees: A genetic interpretation. Sedimentary Geology, 15, 213-233. DOI: 10.1016/0037-0738(76)90017-8

Richter, C., van der Pluijm, B., Housen, B., 1993. The quantification of crystallographic preferred orientation using magnetic anisotropy. Journal of Structural Geology, 15, 113-116.

Robion, P., Frizon de Lamotte, D., Kissel, C., Aubourg, C., 1995. Tectonic versus mineralogical contribution to the magnetic fabrics of epimetamorphic slaty rocks: an example from the Ardennes Massif (France-Belgium). Journal of Structural Geology, 17, 1111-1124.

Robion, P., Kissel, C., Frizon de Lamotte, D., Lorand, J.P., Guézou, J.C., 1997. Magnetic mineralogy and metamorphic zonation in the Ardennes Massif (France-Belgium). Tectonophysics, 271, 231-248.

Robion, P., Averbuch, O., Sintubin, M., 1999. Fabric development and metamorphic evolution of lower Palaeozoic slaty rocks from the Rocroi massif (French–Belgian Ardennes): new constraints from magnetic fabrics, phyllosilicate preferred orientation and illite crystallinity data. Tectonophysics, 309, 257-273.

Robion, R., Grelaud, S., Frizon de Lamotte, D., 2007. Prefolding magnetic fabrics in fold-and-thrust belts: Why the apparent internal deformation of the sedimentary rocks from the Minervois basin (NE - Pyrenees, France) is so high compared to the Potwar basin (SW-Himalaya). Sedimentary Geology, 196, 181-200.

Saez, A, 1987, Estratigrafia y sedimentologia de las formaciones lacustres del tránsito Eoceno-Oligoceno del NE de la Cuenca del Ebro. PhD Thesis. Barcelona (Spain), Universitat de Barcelona, 353pp.

Saez, A., Anadon, P., Herrero, M.J., Moscariello, A., 2007. Variable style of transition between Paleogene fluvial fan and lacustrine systems, southern Pyrenean foreland, NE Spain. Sedimentology, 54, 367-390.

Sagnotti, L., Speranza, S., 1993. Magnetic fabrics analysis of the Plio-Pleistocene clayey units of the Sant' Arcangelo basin, Southern Italy. Physics of the Earth and Planetary Interiors, 77, 165-176.

Sagnotti, L., Winkler, A., Montone, P., Di Bella, L.D., Florindo, F., Mariucci, M.T., Marra, F., Alfonsi, L., Frepoli, A., 1999. Magnetic anisotropy of Plio-Pleistocene sediments from the Adriatic margin of the northern Apennines (Italy): implications for the time-space evolution of the stress field. Tectonophysics, 311, 139-153.

Saint-Bezar, B., Hebert, R.L., Aubourg, C., Robion, P., Swennen, R., Frizon de Lamotte, D., 2002. Magnetic fabric and petrografic investigation of hematite-bearing sandstones within ramp-related folds: examples from the Southern Atlas Front (Morocco). Journal of Structural Geology, 24, 1507-150.

Sans, M., 2003. From thrust tectonics to diapirism: the role of evaporites in the kinematic evolution of the eastern South Pyrenean front. Geologica Acta, 1, 239-259.

Sans, M., Vergés, J., 1995. Fold development Related to Contractional Salt Tectonics: Southeastern Pyrenean Thrust Front, Spain. In: Jackson, M.P.A., Roberts, D.G., Snelson, S. (eds.). Salt tectonics: a global perspective. American Association of Petroleun Geologists Memoir, 369-378.

Sans, M., Muñoz, J.A., Vergés, J., 1996. Triangle zone and thrust wedge geometries related to evaporitic horizons (Southern Pyrenees). Canadian Petroleum Geology Bulletin, 4, 375-384.

Sans, M., Vergés, J., Gomis, E., Parés, J.M., Schiattarella, M., Travé, F.A., Calvet, F., Santanach, P., Doulcet, A., 2003. Layer parallel shortening in salt-detached folds: constraint on cross-section restoration. Tectonophysics, 372, 85-104.

Schmidt, V., Hirt, A.M., Leiss, B., Burlini, L., Walter, J., 2009. Quantitative correlation of strain, texture and magnetic anisotropy of compacted calcite-muscovite aggregates. Journal of Structural Geology, 31, 1062-1073. DOI: 10.1016/j.jsg.2008.11.012

Solé-Sugrañes, L., Mascareñas, P., 1970. Sobre las formaciones Ager y Bagà, del Eoceno del Cadí (Perpirineo oriental) y de unos pretendidos olistolitos del mismo. Acta Geologica Hispanica, 4, 97-101.

Sorby, 1908. On the application of quantitative methods to the structure and history of rocks. Geological Society of London Quaterly Journal, 64, 171-233.

Soto, R., Larrasoaña, J.C., Arlegui, L.E., Beamud, E., Oliva-Urcia, B., Simón, J.L., 2009. Reliability of magnetic fabrics of weakly deformed mudrocks as a palaeostress indicator in compressive settings. Journal of Structural Geology, 31, 512-522.

Souqué, C., Robion, P., Frizon de Lamotte, D., 2002. Cryptic magnetic fabric of tectonic origin revealed by heating of sedimentary samples from the Corbières, France. Physics and Chemistry of the Earth, Parts A/B/C, 27, 1253-1262.

Stacey, F.D., Joplin, G., Lindsay, J., 1960. Magnetic anisotropy and fabric of some foliated rocks from S.E. Australia. Geofisica pura e applicata, 47, 30-40.

Suppe, J., Sàbat, F., Muñoz, J.A., Poblet, J., Roca, E., Vergés, J., 1997. Bed-by-bed fold growth by kink-band migration: Sant Llorenc¸ de Morunys, eastern Pyrenees. Journal of. Structural Geology, 19, 443-461. DOI: 10.1016/S0191764 8141(96)00103-4

Tarling, D.H., Hrouda, F., 1993. The magnetic anisotropy of rocks. London, Chapman and Hall, 217pp.

Tauxe, L., 1998. Paleomagnetic Principles and Practice. Kluwer Academic Publishers, 299pp.

Tavani, S., Storti, F., Salvini, F., 2006. Double-edge fault-propagation folding: geometry and kinematics. Journal of Structural Geology, 28, 19-35.

Tavani, S., Storti, F., Salvini, F., Toscano, C., 2008. Stratigraphic versus structural control on the deformation pattern associated with the evolution of the Mt. Catria anticline, Italy. Journal of Structural Geology, 30, 664-681.

Tavani, S., Mencos, J., Bausà, J., Muñoz, J.A., 2011. The fracture pattern of the Sant Corneli Bóixols oblique inversion anticline (Spanish Pyrenees). Journal of Structural Geology, 33, 1662-1680.

Tavani, S., Storti, F., Lacombe, O., Corradetti, A., Muñoz, J.A., Mazzoli, S., 2015. A review of deformation pattern templates in foreland basin systems and fold-and-thrust belts: Implications for the state of stress in the frontal regions of thrust wedges. Earth-Science Reviews, 141, 82-104.

Teixell, A., 1996. The Ansó transect of the southern Pyrenees: basement and cover thrust geometries. Journal of Geophysical Research, 102, 20,325-20,342.

Teletzke, A.L., Parés, J.M., Kodama, K.P., Anastasio, D.J., 2011. Unsteady deformation along the southwest Spanish Pyrenean thrust front. American Geophysical Union Fall Meeting Abstract, T51B-2321.

Teletzke, A., 2012. Sedimentary and tectonic evolution of the Peña flexure, southwest Pyrenean mountain front, Spain. Theses and Dissertations, Paper 1305, Lehigh University, 68pp.

Thompson, R.J., 1981. The nature and significance of large 'blind' thrusts within the northern Rocky mountains of Canada. In: McClay, K.R., Price, N.J. (eds.). Thrust and Nappe Tectonics. The Geological Society of London, Special Publications (Black- well Scientific Publications, Oxford), 9, 449-62.
Vergés, J., 1993. Estudi geologic del vessant sud del Pirineu oriental i central. Evolucio 1050 cinemàtica en 3D. PhD Thesis. Barcelona (Spain), Universitat de Barcelona, 203pp.
Vergés, J., Martínez, A., Muñoz, J.A., 1992. South Pyrenean fold and thrust belt: The role of foreland evaporitic levels in thrust geometry. In: McClay, K. (ed.). Thrust Tectonics. London, Chapman and Hall, 255-264.
Weil, A.B., Yonkee, A., 2009. Anisotropy of magnetic susceptibility in weakly deformed red beds from the Wyoming salient, Sevier thrust belt: Relations to layer-parallel shortening and orogenic curvature. Lithosphere, 1, 235-256.
Williams, G., Chapman, T., 1983. Strains developed in the hanging walls of thrusts due to their slip/propagation rate: a dislocation model. Journal of Structural Geology, 5, 563-571.
Williams, E.A., Ford, M., Vergés, J., Artoni, A., 1998. Alluvial gravel sedimentation in a contractional growth fold setting, Sant Llorenç de Morunys, southestern Pyrenees. Geological Society of London, 134 (Special Publications), 69-106.
Woodward, N.B., Grey, D.R., Spears, D.B., 1986. Including strain data in balanced cross-sections. Journal of Structural Geology, 8, 313- 324.
Yonkee, A., Weil, A.B., 2009. Reconstructing the kinematic evolution of curved mountain belts: Internal strain patterns in the Wyoming salient, Sevier thrust belt, U.S.A. Geological Society of America Bulletin, 122, 24-49.

Manuscript received November 2017;
revision accepted April 2018;
published Online November 2018.